

A. S. FOUDA¹,
AHMED ABDEL NAZEER²,
E. A. ASHOUR²

paper
UDC :

Amino acids as environmentally-friendly corrosion inhibitors for Cu10Ni alloy in sulfide-polluted salt water: Experimental and theoretical study

The inhibition effect of three amino acids (valine (val), alanine (ala) and glycine (gly)) on the corrosion of Cu10Ni alloy in sulfide-polluted salt water (3.5 % NaCl + 16 ppm S²⁻) was studied using potentiodynamic polarization, electrochemical impedance spectroscopy (EIS), electrochemical frequency modulation (EFM), scanning electron microscopy (SEM) and energy dispersive X-ray diffraction (EDX). The polarization measurements showed that the tested compounds act as mixed-type inhibitors. Results obtained from the different techniques reveal that the inhibition efficiency (%IE) follows the sequence: val > ala > gly. A synergistic effect was observed between these inhibitors and KI. SEM showed a remarkable inhibiting effect of these additives due to the protective film formed on the alloy surface confirmed by the presence of the carbon and nitrogen atoms in the EDX spectra. The adsorption of these inhibitors was found to be of a physisorption mode and obeys Langmuir's adsorption isotherm. Some quantum chemical parameters were calculated by the MNDO Semi-empirical method to provide further insight into the mechanism of inhibition of the corrosion process.

Key words: Corrosion inhibition, Cu10Ni alloy, amino acids, NaCl, Na₂S

INTRODUCTION

Copper and copper-based alloys are being used in structures and components that are usually exposed to seawater and other marine environments. This is due to their high corrosion resistance, ease of workability and good heat transfer properties. The corrosion resistance of these alloys in seawater is related to the nature of the formed protective corrosion product film [1]. North and Pryor [2] found that the protective film is largely cuprous oxide (Cu₂O) with cuprous hydroxy chloride (Cu₂(OH)₃Cl) and cupric oxide (CuO) being present in significant amounts.

Inspite of this self-protective effect, copper and its alloys may suffer damaging effects in different environments. For example, chloride ions are known to be very aggressive to copper and its alloys due to the tendency of the chloride ion to form an unstable film, CuCl, as well as soluble chloride complexes such as CuCl₂⁻, CuCl₃⁻² [3, 4]. Therefore, trace amounts of Cl⁻ ions can cause corrosion problems to copper and its alloys. Also, the presence of sulfide in the seawater from seaweed, sulfide reducing bacteria, or industrial waste discharge is known to promote aqueous corrosion of copper and its alloys [5]. It was found that corrosion rate of Cu-based alloys increases

by a factor of 10-30 when being used in seawater that contains sulfur compounds as impurities [6]. Mac Donald et al [7], have suggested that the presence of sulfide ions in deoxygenated chloride medium accelerates the corrosion rate of Cu-Ni alloys. Eldomiaty and Alhajji [8], reported that the general corrosion of Cu-Ni alloys in low (<100ppm) and high (>100ppm) sulfide polluted seawater increases due to the selective copper dissolution. Sayed et al. [9] have studied the effect of dealloying of Cu-Ni alloys in chloride environment containing 500 and 1000ppm of sulfide and showed the strong dependence of the extent of corrosion attack of Cu-Ni alloys on the concentration of sulfide ions. The presence of sulfide ions in seawater is found to influence the fatigue strength and fatigue life of Al-brass and Cu10Ni alloys [10], the susceptibility of Al-bronze to stress corrosion cracking [11, 12] and the corrosive wear of copper alloys [13].

Literature survey reveals that a wide variety of organic compounds are being used as inhibitors against the corrosion of copper and its alloys [14-22]. Although benzotriazole (BTA) and its derivatives are known to be very effective corrosion inhibitors for copper and its alloys over a wide temperature and pH range, they are toxic materials [23, 24].

Therefore, there is some researches were developed to use environmentally friendly corrosion inhibitors which are cheap and can be safely handled [25-32]. Amino acids are relatively cheap, non toxic,

Address authors: ¹Department of Chemistry, Faculty of Science, El-Mansoura University, El- Mansoura-35516, Egypt, ²Electrochemistry and Corrosion Lab., National Research Centre, Dokki, Cairo-12622, Egypt.

and completely soluble in aqueous media. Consequently, there are many reports recently on the use of different amino acids as corrosion inhibitors for vanadium [33], copper [22, 27, 34-40], copper-nickel alloys [41], steel [42-45], and aluminum [26] in various corrosive environments.

The present work aims to characterize the effect of three amino acids (valine, alanine, and glycine) as corrosion inhibitors for Cu10Ni alloy in sulfide polluted salt water, synergistic effect of KI and surface examination were also studied. The relationship between calculated quantum chemical parameters and experimental inhibition efficiencies of the amino acids was also discussed.

2. EXPERIMENTAL

2.1. Materials

Tests were performed on a commercial Cu10Ni alloy specimen of the following composition (weight %): 87.57 Cu, 10.68 Ni, 1.2 Fe and 0.55 Mn, which was provided by Abu-Queer Power Station, Alexandria, Egypt.

2.2. Solutions

Solutions were prepared from Analytical grade chemicals and doubly distilled water. Na₂S was obtained from Ridel- de Haen while valine, alanine and glycine were obtained from Aldrich chemical Co. Ltd. All measurements were performed in solutions containing 3.5 % NaCl which have a comparable salt level to that of seawater. Double distilled water was used in all preparations.

2.3. Potentiodynamic polarization measurements

The potentiodynamic polarization measurements were performed in a conventional three-electrode glass cell with working volume of 100ml using a PGZ100 Volta Lab potentiostat (Radiometer Analytical S.A.). A working electrode was a sheet with dimension 1x1 cm and welded in a Cu wire from one side for connection and fixed in polytetrafluoroethylene (PTFE) rods by epoxy resin in such a way that only one surface; of area 1cm² was left uncovered. Before experiments the electrode surface was polished mechanically and treated in the way as described before. A Pt counter electrode and a saturated calomel electrode (SCE) as reference electrode were used. Polarization measurements were performed at potentials from -450 mV to -150 mV at a scan rate of 0.33 mVs⁻¹ after steady state potential had been established in cathodic or anodic direction. All measurements were carried out in deoxygenated solution of 3.5% NaCl with and without addition of 16 ppm of sulfide ions in the absence and presence of different concentrations of inhibitors. The experimental results

were reproducible and each experiment was carried out at least twice.

2.4. Electrochemical impedance spectroscopy (EIS)

The impedance measurements were performed using an ac signal with amplitude 10 mV in the frequency range from 2x10⁴ Hz to 0.05 Hz. The spectra were recorded under open circuit conditions after 30 min. exposure in the test solution.

2.5. Electrochemical Frequency Modulation Technique (EFM)

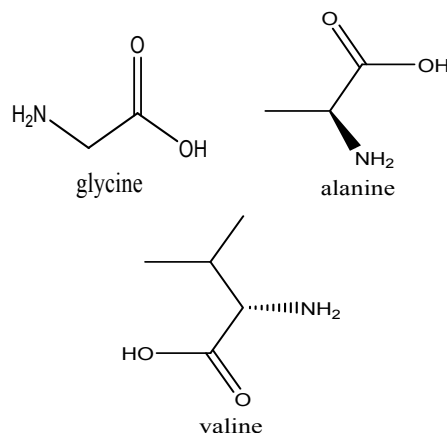
The EFM data have been analyzed using Echem analyst 5.21 for results plotting, graphing data fitting & calculating. In this technique applying potential perturbation signal with amplitude of 10 mV with two sine waves of 2 and 5 Hz occurs. The intermodulation spectra contain current responses assigned for harmonical and intermodulation current peaks. The larger peaks were used to calculate the corrosion current density (i_{corr}), the Tafel constants (β_a and β_c) and the causality factors CF-2 and CF-3.

2.6. SEM-EDS measurements

The electrode surfaces of Cu10Ni were analyzed by scanning electron microscope – type JOEL 840, Japan before and after immersion in polluted test solutions in the absence and presence of the optimum concentration of the amino acids at 25 °C, for 35 days immersion time. The specimens were washed gently with water, then dried carefully and examined without any further treatments.

2.7. Quantum calculations

Quantum-chemical calculations were carried out using of semi-empirical method (MNDO). The following quantum chemical indices were calculated for the investigated compounds: the energy of the highest occupied molecular orbital (E_{HOMO}), the energy of the lowest unoccupied molecular orbital (E_{LUMO}), energy gap ($\Delta E = E_{LUMO} - E_{HOMO}$), dipole moment (μ), and Mulliken charges.



Chemical structure of the investigated amino acids.

3. RESULTS AND DISCUSSION

3.1. The potentiodynamic polarization

The potentiodynamic polarization curves of Cu10Ni alloy in sulfide polluted salt water (3.5 % NaCl + 16 ppm S²⁻) with different concentrations of alanine are shown in (Figure 1). From this figure, it is

evident that in the presence of alanine, shifts the potential towards more positive potential region and the shift was found to be dependent on inhibitor concentration. Similar curves were obtained for glycine and valine (not shown). The current density also decreased with increasing concentration of the inhibitors.

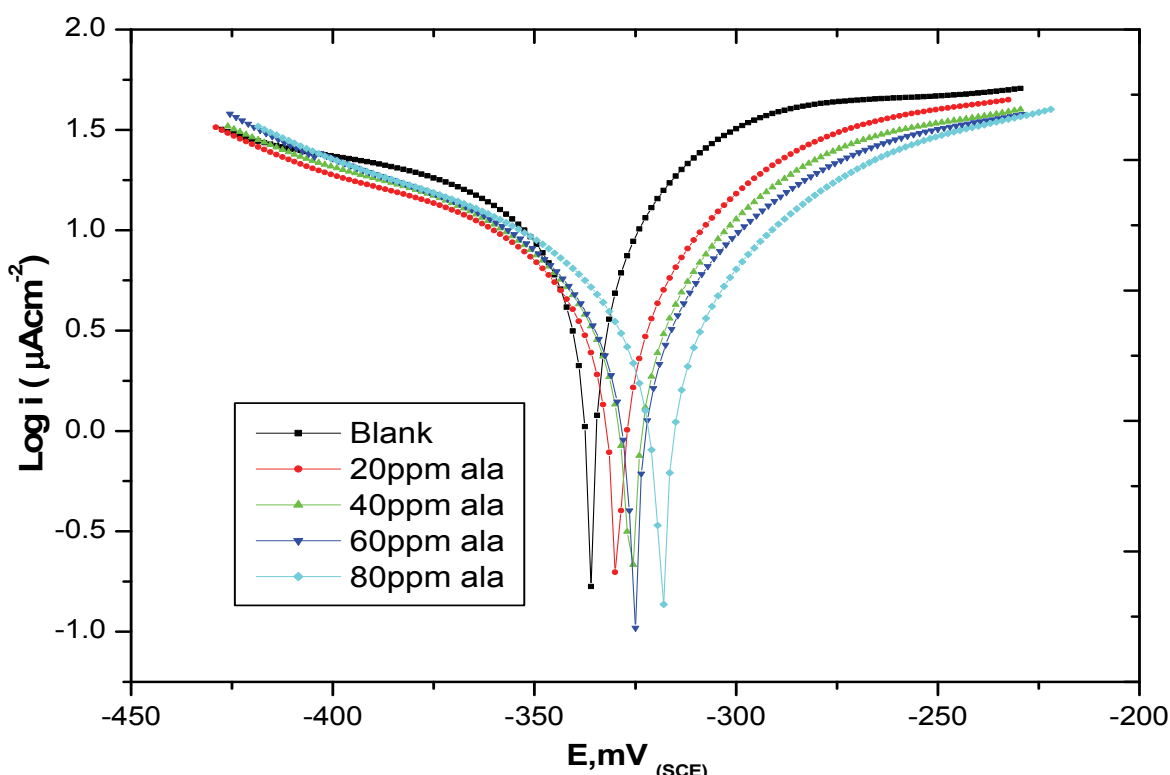


Figure 1 - Polarization curves of Cu10Ni alloy in 3.5% NaCl + 16 ppm sulfide (blank) + different concentrations of alanine.

The corrosion rate [46] and the inhibition efficiency [47] were calculated from polarization curves using the following equations:

$$CR = \frac{3.27 \times 10^{-3} \times i_{corr} \times EW}{D} \quad (1)$$

$$IE\% = \frac{[i_{corr} - i_{corr(inh)}]}{i_{corr}} \times 100 \quad (2)$$

where CR is the corrosion rate (mm year⁻¹), D the density (g cm⁻³), EW the equivalent weight of the specimen and $i_{corr(inh)}$ and i_{corr} are the corrosion current density ($\mu A cm^{-2}$) values with and without inhibitor, respectively. These were determined by extrapolation

of the Tafel lines and the open circuit potential of the corresponding polarization curves.

The values of different electrochemical parameters are summarized in Table 1. The addition of these inhibitors slows down the rate of both partial corrosion reactions without shifting the corrosion potential (E_{corr}). This means that these inhibitors act as mixed-type inhibitors. The cathodic and anodic Tafel slopes (β_c, β_a) do not change significantly in the presence of inhibitors. This fact suggests that these compounds do not change the kinetics of hydrogen evolution and alloy dissolution.

The inhibition efficiency of these amino acids increases with increase in concentration (Table 1). The order of the inhibition efficiency is: valine > alanine > glycine.

Table 1 - Electrochemical parameters obtained from potentiodynamic polarization measurements of Cu10Ni alloy in (3.5% NaCl + 16 ppm S²⁻) in the absence and presence of various concentrations of glycine, alanine and valine at 25°C

Conc., ppm	$i_{corr.}$, $\mu\text{A cm}^{-2}$	$-E_{corr.}$, mV	β_c , mV dec. ⁻¹	β_a , mV dec. ⁻¹	θ	%IE	R_p	corrosion rate (CR) mm/year
Blank	9.65	336.0	-145.2	69.3	0.00	0.00	2.5	112.9
20 ppm glycine	7.07	329.0	-111.7	71.3	0.267	26.7	1.89	82.79
40 ppm glycine	5.86	323.1	-101.2	70.5	0.393	39.3	2.2	68.58
60 ppm glycine	4.94	301.0	-101.4	59.9	0.488	48.8	2.46	57.82
80 ppm glycine	4.61	290.9	-121.8	52.6	0.522	52.2	2.56	53.92
20 ppm alanine	4.96	329.5	102.8	62.1	0.486	48.6	2.54	58.08
40 ppm alanine	3.97	326.1	81.2	58.0	0.589	58.9	2.80	46.29
60 ppm alanine	3.70	325.0	74.2	61.6	0.617	61.7	2.95	43.37
80 ppm alanine	3.54	318.2	79.2	61.2	0.633	63.3	3.15	41.40
20 ppm valine	4.24	328.0	-109.3	60.9	0.561	56.1	2.46	50.32
40 ppm valine	3.31	322.9	-81.9	58.5	0.657	65.7	3.34	38.50
60 ppm valine	2.75	320.3	-74.1	60.6	0.715	71.5	3.21	34.79
80 ppm valine	2.07	316.2	-70.8	57.9	0.786	78.6	4.82	25.56

3.2. Effect of iodide ion addition

It has been reported that the presence of negative ions, like iodide, may enhance the adsorption of amino acids on substrates [48]. Therefore, the corrosion inhibition of Cu10Ni alloy in sulfide polluted saltwater in presence of 100 ppm KI with different

concentrations of the amino acids was studied using potentiodynamic measurements. Figure 2 shows the polarization curves for Cu10Ni alloy in polluted seawater in the absence and presence of 100 ppm KI with different concentrations of Ala.

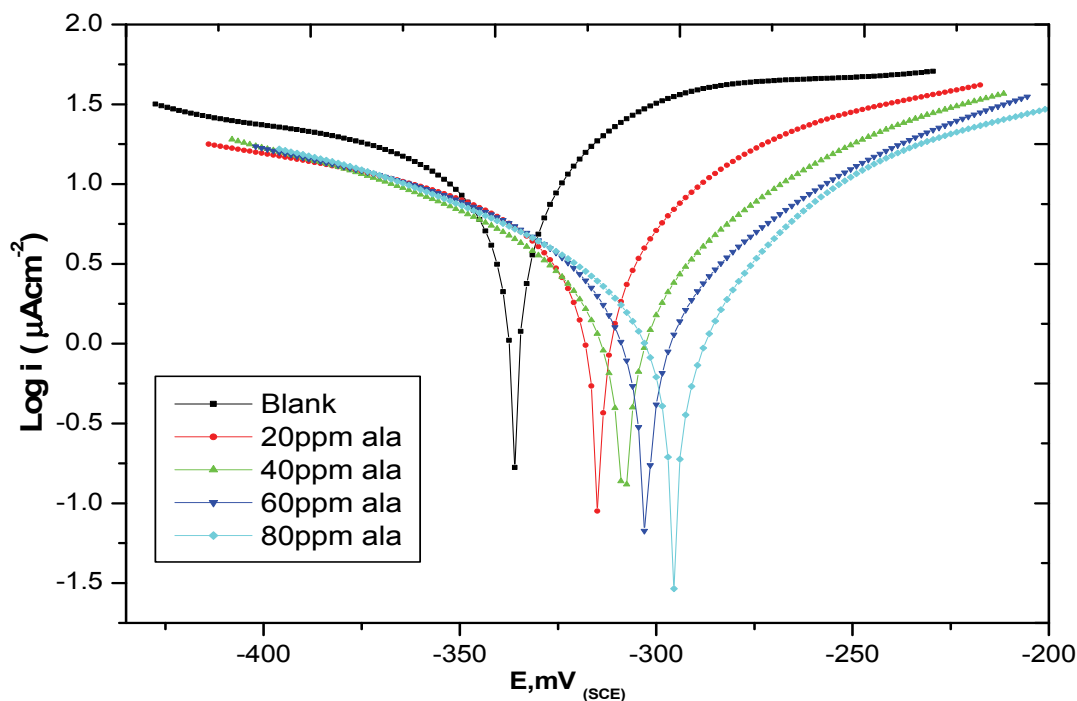


Figure 2 - Polarization curves of Cu10Ni alloy in 3.5% NaCl+16 ppm sulfide (blank) alone and with 100 ppm KI in presence of different concentrations of alanine.

The values of inhibition efficiencies (% IE) for various concentrations of inhibitors in the absence and presence of 100 ppm KI are given in Table 2. Note that the inhibition efficiency of 80 ppm of valine, alanine, and glycine attains a maximum value of 78.6, 63.3 and 52.2%, respectively. The addition of 100 ppm KI to these amino acids enhances the inhibition efficiency significantly up to 86.0, 83.1 and 79.6%, respectively. This synergistic effect is found to increase

with increasing the concentration of the amino acids. The strong chemisorption of iodide ion on the metal surface is responsible for the synergistic effect of this anion in combination with cations of the inhibitor. The cation is then adsorbed by coulombic attraction on the metal surface where this anion is already adsorbed by chemisorption. Stabilization of this adsorbed anion with cations leads to greater surface coverage and therefore greater inhibition efficiency.

Table 2 - Electrochemical parameters obtained from potentiodynamic polarization measurements of Cu10Ni alloy in (3.5% NaCl + 16 ppm S²⁻) in absence and presence of 100 ppm KI + various concentrations of glycine, alanine and valine at 25°C.

Conc., ppm	i _{corr.} , $\mu\text{A cm}^{-2}$	-E _{corr.} , mV	β_c , mV dec. ⁻¹	β_a , mV dec. ⁻¹	θ	%IE	R _p	corrosion rate (CR) mm/year
Blank	9.65	336.0	-145.2	69.3	0.00	0.00	2.5	112.9
20 ppm glycine + 100 ppm KI	4.16	319.5	-109.2	66.7	0.569	56.9	3.04	48.69
40 ppm glycine + 100 ppm KI	3.00	316.3	-65.4	53.4	0.689	68.9	4.78	35.11
60 ppm glycine + 100 ppm KI	2.52	305.1	-51.7	55.6	0.739	73.9	5.57	29.50
80 ppm glycine + 100 ppm KI	1.97	301.2	-42.3	60.9	0.796	79.6	8.08	23.06
20 ppm alanine + 100 ppm KI	3.83	314.8	-110.7	62.7	0.603	60.3	3.39	44.77
40 ppm alanine + 100 ppm KI	2.35	308.2	-73.0	56.8	0.756	75.6	5.63	27.51
60 ppm ala + 100 ppm KI	1.98	302.6	-63.0	55.7	0.795	79.5	6.15	23.17
80 ppm alanine + 100 ppm KI	1.63	295.8	-80.2	50.1	0.831	83.1	6.57	19.02
20 ppm valine + 100 ppm KI	3.65	325.5	-89.4	66.3	0.622	62.2	3.27	42.77
40 ppm valine + 100 ppm KI	2.03	319.3	-67.7	57.9	0.790	79.0	5.16	23.76
60 ppm valine + 100 ppm KI	1.62	311.4	-63.1	57.4	0.832	83.2	5.93	18.95
80 ppm valine + 100 ppm KI	1.35	300.3	-64.3	50.6	0.860	86.0	6.93	15.85

3.3. Electrochemical impedance spectroscopy

The Nyquist plots of Cu10Ni alloy in sulfide polluted salt water in the absence and presence of the optimum concentration of alanine alone and with KI are given in Figure 3. Similar Figures were obtained for valine and glycine (not shown). A depressed semi-circular shape with their centers below the real axis was obtained. This behavior is typical for solid metal electrodes that show frequency dispersion of the impedance data [49]. The corrosion behavior of Cu10Ni alloy in the uninhibited solutions was influenced by mass transport. This Figure shows that Warburg diffusion impedance possibly exists in the absence of the amino acids.

From Fig. 3, it can be noticed that the Warburg impedance disappears and the impedance response of Cu10Ni alloy significantly changes in shape and size by addition of glycine, alanine and valine alone and with KI. Also, the impedance response increased in

the presence of the inhibitors. The presence of the inhibitors and KI in sulfide polluted salt water solution change the mechanism of corrosion of Cu10Ni or at least may hinder the charge transfer from the Cu10Ni alloy surface.

The equivalent circuits employed for this system are presented in Fig. 4. The first equivalent circuit [Figure 4 (a)] was used to stimulate the EIS data displaying a Warburg impedance in uninhibited medium, while the second [Figure 4 (b)] was used to fit the EIS data displaying a capacitive semicircle in case of the inhibited solutions. Note that R_s is the solution resistance, R_{ct} is the charge transfer resistance, W is the Warburg impedance and CPE is the constant phase element whose impedance is given by:

$$Z_{CPE} = Y_o^{-1}(j\omega)^n \quad (3)$$

where Y_o is the constant phase element (CPE) of the electrical double layer, j is an imaginary number, $\omega =$

$=2\pi f$ is the angular frequency (rad/s), f is the frequency of the applied signal, n is the CPE exponent for whole number of $n = 1, 0, -1$ CPE is reduced to the capacitor (C), resistance (R) and inductance (L) respectively. The value of $n = 0.5$ corresponds to Warburg impedance (W). The dispersion of the capacitive semicircle is related to surface heterogeneity

due to surface roughness or inhibitor adsorption and formation of porous layer [50]. Thus, n serves as a measure of surface heterogeneity. Considering that the impedance of a double layer does not behave as an ideal capacitor, CPE is most often used to describe the frequency dependence of non ideal capacitive behavior [51].

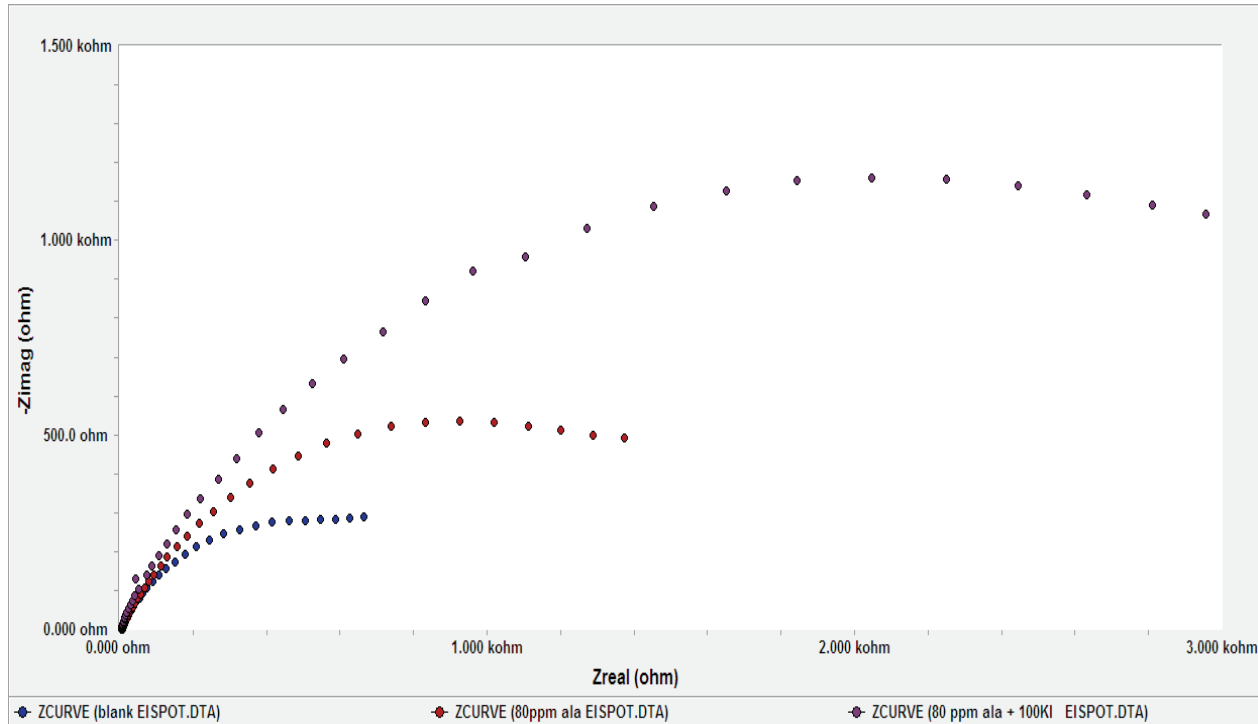


Figure 3 - Electrochemical impedance spectra for Cu10Ni alloy in 3.5% NaCl + 16ppm S^{2-} solution containing 80 ppm alanine alone and with 100 ppm KI.

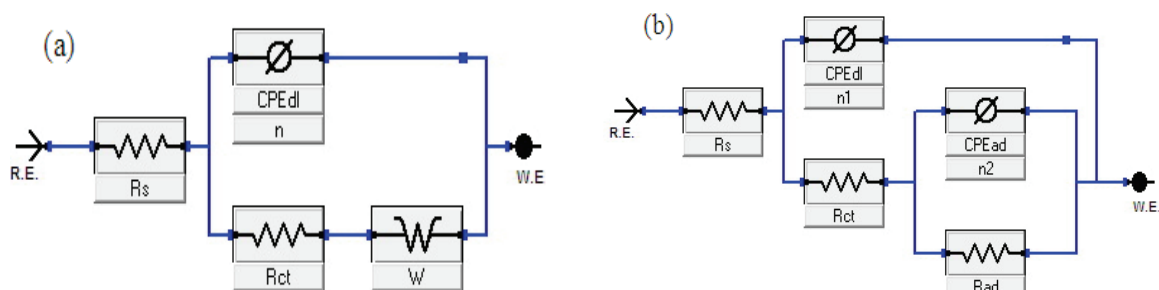


Figure 4 - Equivalent circuits used to fit the experimental EIS data.

The inhibition efficiency (IE %) of the three inhibitors alone and with 100 ppm KI was calculated from the following equation:

$$IE_{EIS} (\%) = [(R_{ct} - R'_{ct}) / R_{ct}] \times 100 \quad (4)$$

where R_{ct} and R'_{ct} are the charge transfer resistance for the inhibited and uninhibited solutions, respectively. From the data in Table 3, we can conclude that the values of the CPE have decreased significantly in

the presence of the optimum concentration of the inhibitors and decreased more in the presence of KI. The decrease in the CPE values may be due to the complex formation at the metal surface which reduces the thickness of the double layer. Therefore, the R_{ct} values have increased indicating the corrosion inhibitive nature of blends [52]. The results of the impedance studies are in agreement with those obtained employing potentiodynamic measurements.

Table 3 - Electrochemical kinetic parameters obtained by EIS technique for Cu10Ni alloy in 3.5%NaCl + 16ppm S²⁻ (blank) in the absence and presence of the optimum concentration of glycine, alanine and valine alone and with 100 ppm KI.

Conc., (M)	R _s (Ω cm ²)	CPE1		R _{ad} (Ω cm ²)	CPE2		W Ω cm ⁻²	% IE
		Y ₀ (μF cm ⁻²)	n1		Y ₀ (μF cm ⁻²)	n2		
blank	6.349	566.4	0.738	724	-	-	6.052	-
blank + 80 ppm glycine	6.486	272.0	0.730	1559	538.0	81.84	-	53.56
blank + 80 ppm alanine	6.585	164.66	0.855	1881	291.1	0.616	-	61.56
blank + 80 ppm valine	6.218	111.2	0.810	3329	236.8	0.597	-	78.25
blank + 80 ppm glycine + +100 ppm KI	6.968	59.91	0.854	3636	254.0	0.597	-	80.01
blank + 80 ppm alanine + +100 ppm KI	5.721	56.69	0.850	4329	150.2	0.520		83.28
blank + 80 ppm valine + +100 ppm KI	7.170	54.40	0.886	5833	133.0	0.528	-	87.6

3.4. Electrochemical frequency modulation

The EFM technique has been used to calculate anodic and cathodic Tafel slopes as well as corrosion current densities for Cu10Ni alloy in sulfide polluted salt water (3.5% NaCl + 16ppm S²⁻) in the absence and presence of the optimum concentrations of the studied amino acids alone and with 100ppm KI,

shown in Figure 5. The larger peaks were used to calculate the electrochemical parameters (corrosion current density (i_{corr}), the Tafel slopes (β_a and β_c) and the causality factors (CF-2 and CF-3)) given in Table 4. The great strength of the EFM is the causality factors which serve as an internal check on the validity of the EFM measurement [53].

Table 4 - Electrochemical kinetic parameters obtained by EFM technique for Cu10Ni alloy in 3.5% NaCl + 16ppm S²⁻ (blank) in absence and presence of the optimum concentration of valine, alanine and glycine alone and with 100ppm KI

Conc., M	i _{corr} , μA cm ⁻²	β_a , mV dec ⁻¹	β_c , mV dec ⁻¹	CF-2	CF-3	IE%	C.R, mpy
blank	21.13	41.59	93.73	1.99	2.84	--	9.62
80 ppm glycine	9.29	22.59	37.25	1.96	2.79	56.06	4.23
80 ppm alanine	6.91	27.20	39.27	2.01	2.82	67.30	3.15
80 ppm valine	4.34	41.34	55.93	1.93	2.91	79.50	1.98
80 ppm glycine + 100 ppm KI	3.86	40.47	54.37	1.748	2.87	81.73	1.75
80 ppm alanine + 100 ppm KI	2.73	29.05	32.50	1.97	2.92	87.09	1.24
80 ppm valine + 100 ppm KI	2.51	25.46	28.94	1.72	2.97	88.11	1.15

From Table 4, one can conclude that the corrosion current densities decrease by increasing the concentration of the amino acids. Also the inhibition efficiencies IE_{EFM} (%), calculated from equation (5), increase by increasing the studied amino acids concentrations.

$$IE_{EFM} (\%) = [(i^0_{corr} - i_{corr}) / i^0_{corr}] \times 100 \quad (5)$$

where i⁰_{corr} and i_{corr} are corrosion current densities in the absence and presence of inhibitors, respectively. Also the causality factors CF-2 and CF-3 are close to their theoretical values of 2 and 3, respectively indicating that the measured data are of high quality [54].

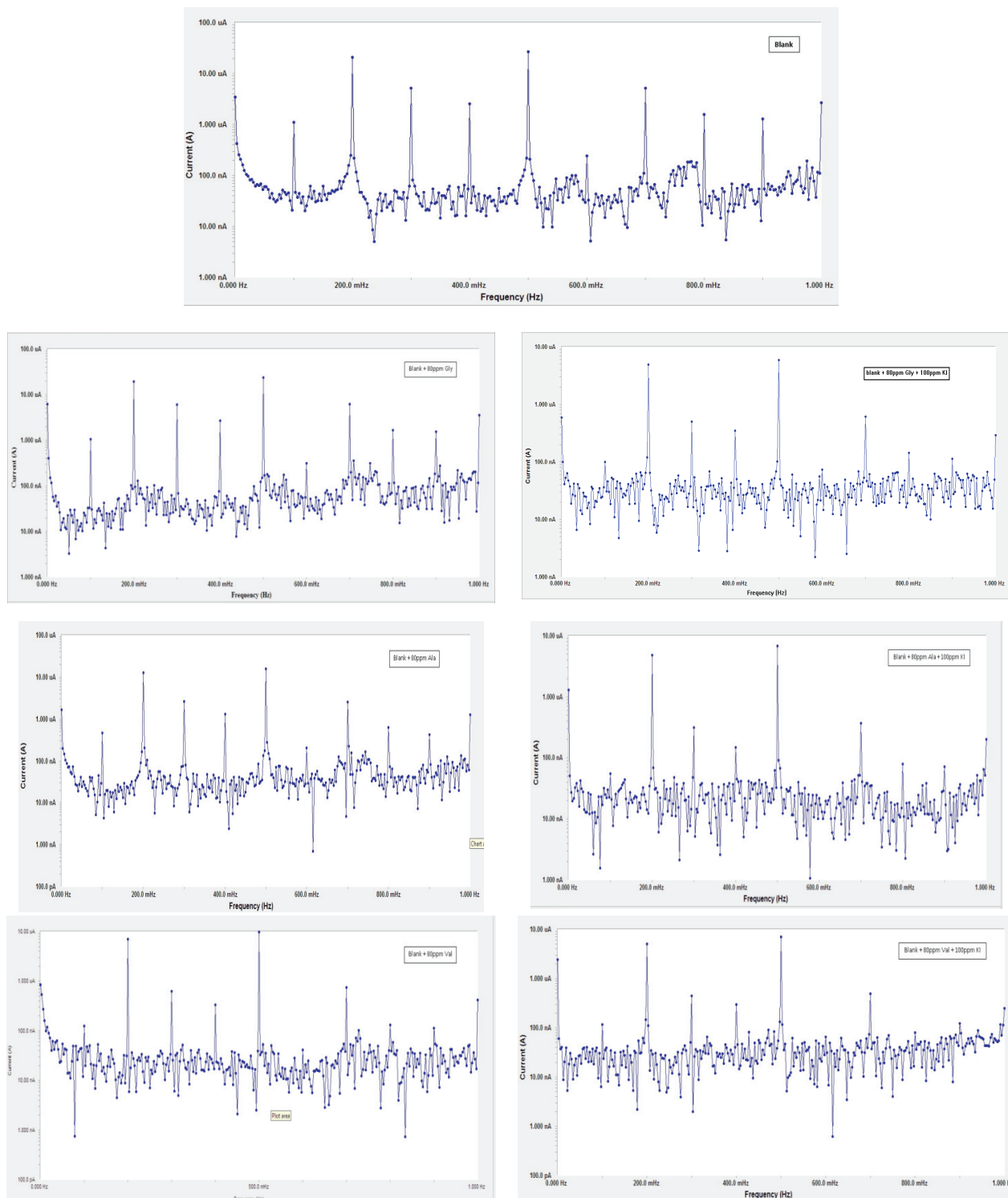


Figure 5 - Intermodulation spectra for Cu10Ni alloy in 3.5% NaCl + 16 ppm S^{2-} (blank) in the absence and presence of the optimum doses of the three amino acids alone and with 100 ppm KI

From the inhibition efficiencies obtained using potentiodynamic polarization, EIS and EFM techniques for corrosion of Cu10Ni alloy in sulfide polluted salt water in the presence of valine, alanine

and glycine alone and with KI, it is obvious that there is a very good agreement between the data obtained from electrochemical techniques and that obtained from EFM technique (Figure 6).

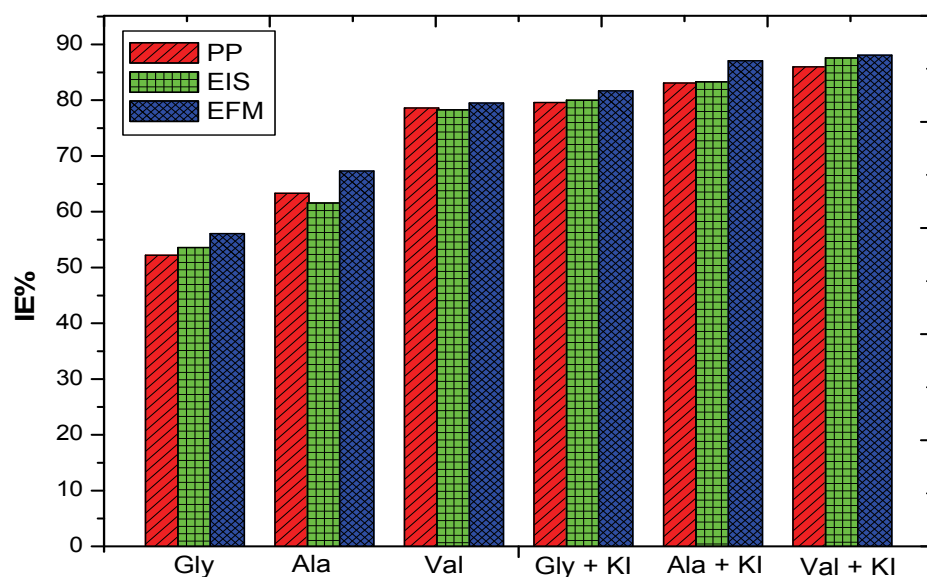


Figure 6 - Comparison of inhibition efficiencies recorded using potentiodynamic polarization (PP), EIS and EFM techniques.

3.5. The adsorption isotherm

In order to get a better understanding of the electrochemical process on the metal surface, it is important to know the mode of adsorption of the amino acids on Cu10Ni alloy that fits the experimental results. The degree of surface coverage (θ) for

different concentrations of the three amino acids in sulfide polluted seawater was evaluated using the inhibition efficiency data ($IE_p/100$). Different adsorption isotherms were tested for agreement with the experimental data.

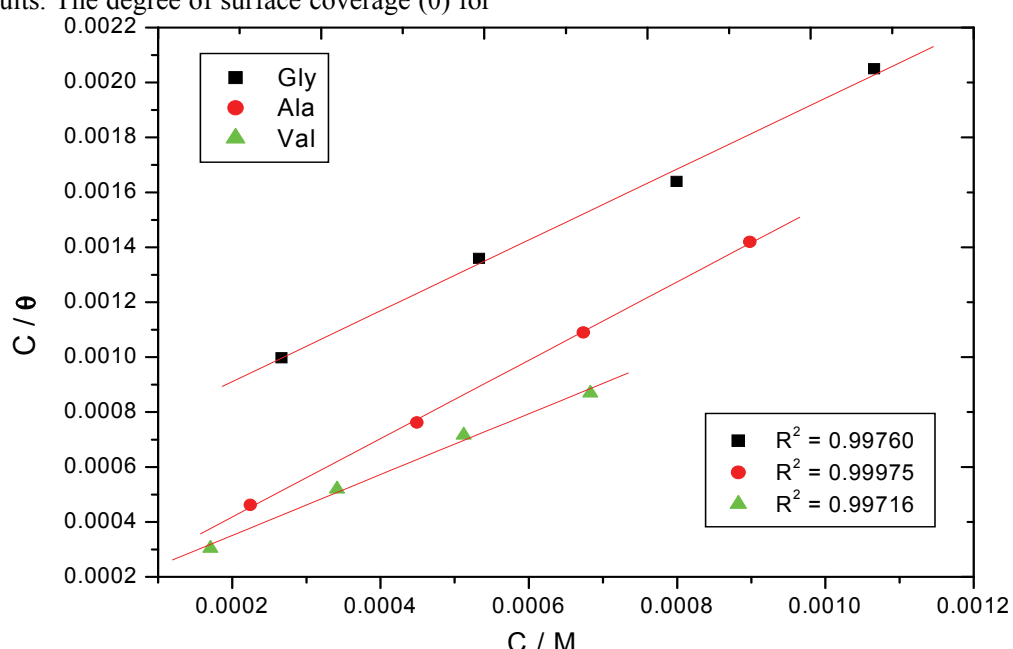


Figure 7 - Langmuir adsorption isotherm for glycine, alanine and valine for corrosion of Cu10Ni alloy in 3.5% NaCl + 16 ppm S^{2-}

The linear relations in the C/θ on C plots for the three amino acids at 25 °C (Figure 7) suggest that the

adsorption of these compounds on Cu10Ni alloy follows Langmuir adsorption isotherm:

$$C / \theta = I / K + C \quad (6)$$

where C is the concentration of inhibitor and K is the adsorption equilibrium constant related to the free energy of adsorption ΔG_{ads} as following [55]:

$$K = I / 55.5 \exp(-\Delta G_{ads}^o / RT) \quad (7)$$

where 55.5 represents the molar concentration of water in mol L⁻¹. The validity of Langmuir's isotherm of these compounds adsorption on Cu10Ni alloy indicates that the interaction forces between the molecules in the adsorbed layer are equal to zero. Higher values of equilibrium constant (K) were obtained for the three compounds (Table 5). This confirms that the adsorption capability of the investigated compounds depends on their donor-acceptor properties (E_{HOMO} and E_{LUMO} values) and also, suggested strong interaction of the inhibitors and the alloy surface [56]. The increasing in K_{ads} reflects the increasing adsorption ability which can be given in the following increasing order: valine > alanine > glycine.

Table 5 - Adsorption coefficients deduced from Langmuir isotherm for valine, alanine and glycine

Inhibitor	Langmuir isotherms			
	K_{ads} , M ⁻¹	Slope	R ²	$-\Delta G_{ads}^o$, kJ mol ⁻¹
glycine	1.5	1.29	0.9976	28.12
alanine	7.5	1.43	0.99975	32.07
valine	7.7	1.11	0.99716	32.12

The free energy of adsorption ΔG_{ads} , for all inhibitors was calculated and recorded in Table 5. The relatively high and negative free energy values may indicate a relatively strong and spontaneous adsorption of the amino acids on Cu10Ni alloy, which explains its high corrosion inhibition efficiency. A value of -40 kJ mol⁻¹ is usually adopted as a threshold value between chemical and physical adsorption [57]. The calculated values of ΔG_{ads} , for valine, alanine and glycine are equal -32.1, -32.1 and -28.1 kJ mol⁻¹ respectively, which means that the adsorption of these inhibitors are physically through electrostatic interaction between the inhibitor and the alloy surface.

3.6. SEM-EDX investigations

SEM and EDS experiments were carried out in order to verify if the amino acid molecules are in fact adsorbed on Cu10Ni alloy surface or just peeled off the surface.

The SEM micrographs for Cu10Ni alloy surface after 35 days immersion in 3.5% NaCl + 16 ppm S²⁻ without and with the addition of the optimum concentration of the three amino acids alone and with 100 ppm KI are shown in Figure 8. From this Figure, it can be seen that the alloy surface is covered by spongy corrosion products in the absence of the

amino acids (Figure 8B). In contrast, in presence of the optimum concentration of the amino acids, the metallic surface seems to be almost not affected by corrosion and some precipitates observed, we believe, because of insufficient surface rinsing. A comparison of SEM micrographs obtained in the absence and in the presence of the inhibitors reveals a marked inhibiting effect of these compounds.

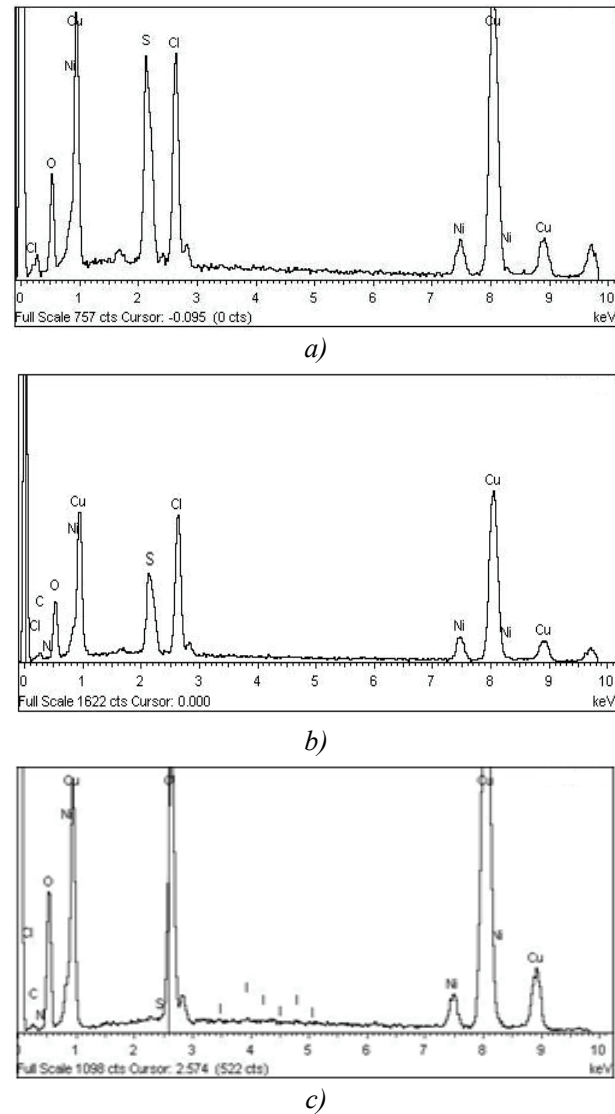


Figure 8 - EDS spectra of Cu10Ni alloy in 3.5% NaCl + 16 ppm S²⁻ in the absence (a), in the presence of 80 ppm alanine (b) and in 80 ppm alanine + 100 ppm KI (c)

The corresponding EDS profile analyses are presented in Table 6 and Figure 9 for alanine and the others amino acids not shown. It is also important to notice the existence of C and N peaks in the EDS spectra of the Cu10Ni alloy surface corresponding to the samples immersed for 35 day in solutions containing the optimum concentration of alanine (Figure 9B), in addition to the existence of iodide ion in the

presence of alanine with KI (Figure 9C), which suggest the adsorption of inhibitors on the electrode

surface. The formation of a thin inhibitor film is in agreement with the SEM observations.

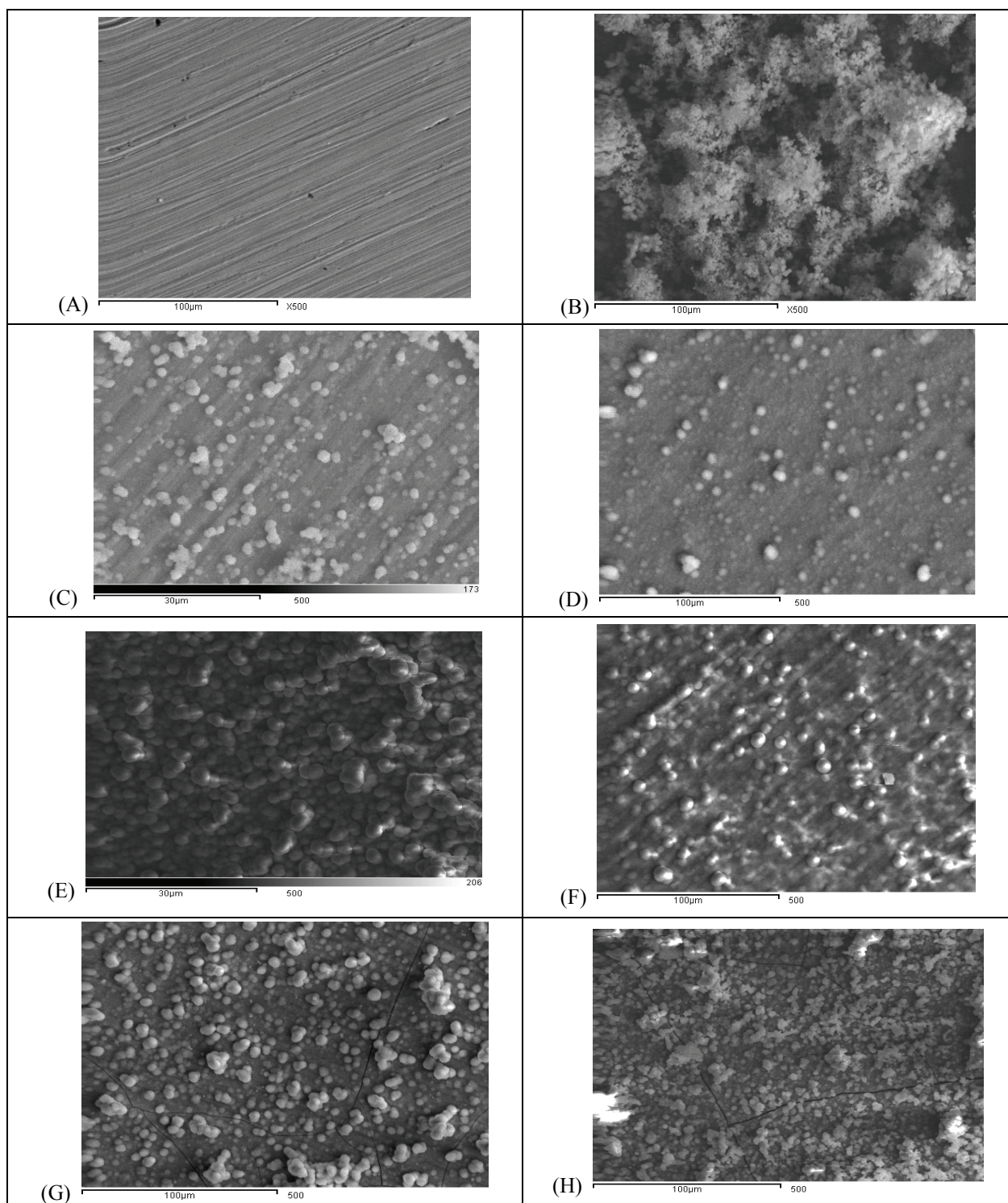


Figure 9 - SEM micrographs of Cu10Ni alloy before and after immersion for 35 days in 3.5% NaCl + 16 ppm S^{2-} (blank) with different concentrations of inhibitors (A) sample without immersion (clean sample), (B) in blank, (C) blank + 80 ppm valnine, (D) blank + 80 ppm valnine + 100 ppm KI, (E) blank + 80 ppm alanine, (F) blank + 80 ppm alanine + 100 ppm KI, (G) blank + 80 ppm glycine and (H) blank + 80 ppm glycine + 100 ppm KI.

Table 6 - Surface composition (wt%) of Cu10Ni alloy after 35 day of immersion in 3.5% NaCl + 16ppm S²⁻ (blank) without and with the optimum concentration of glycine, alanine and valine alone and with 100ppm KI.

(Mass %)	Cu	Ni	Cl	S	O	C	N	I
blank	43.15	3.93	17.90	9.85	25.17	-	-	-
80 ppm glycine	41.51	2.78	15.67	3.98	30.58	3.60	1.88	-
80 ppm alanine	44.34	2.92	11.34	1.26	32.83	4.80	2.51	-
80 ppm valine	47.12	3.04	11.14	1.15	30.15	4.85	2.55	-
80 ppm glycine + 100 ppm KI	48.10	2.68	12.31	0.24	29.34	4.04	2.27	1.02
80 ppm alanine + 100 ppm KI	49.11	3.13	10.92	0.06	27.87	4.91	2.72	1.28
80 ppm valine + 100 ppm KI	53.56	3.82	6.74	0.66	24.18	5.62	3.50	1.92

3.7. Quantum chemical calculation using semiempirical method (MNDO)

Over the past decades the semiempirical molecular orbital methods have been widely used in computational studies. Semiempirical methods serve as efficient computational tools which can yield fast quantitative estimates for a number of properties [58]. MNDO (modified neglect of differential overlap) is a semiempirical method based on the NDDO (neglect of diatomic differential overlap) approximation.

Highest occupied molecular orbital energy (E_{HOMO}) and lowest unoccupied molecular orbital energy (E_{LUMO}) are very popular quantum chemical parameters. These orbitals, also called the frontier orbitals, determine the way the molecule interacts with other species. According to the frontier molecular orbital theory, the formation of a transition state is due to an interaction between the frontier orbitals (HOMO and LUMO) of reactants [59]. E_{HOMO} is often associated with the electron donating ability of the molecule. High E_{HOMO} values indicate that the molecule has a tendency to donate electrons to appropriate acceptor molecules with low energy empty molecular orbital. Increasing values of the E_{HOMO} facilitate adsorption (and therefore inhibition) by influencing the transport process through the adsorbed layer [60, 61]. E_{LUMO} indicates the ability of the molecules to accept electrons. The lower values of the E_{LUMO} , the more probable it is that the molecule would accept electrons. A low value of the energy band gap ($\Delta E = E_{LUMO} - E_{HOMO}$) gives good inhibition efficiencies, because the energy to remove an electron from the last occupied orbital will be low [62]. Also low value of the dipole moment (μ) will favour the accumulation of inhibitor molecules on the metallic surface.

Evaluation of the efficiency of valine, alanine and glycine as corrosion inhibitors for Cu10Ni alloy in sulfide polluted salt water has been performed using MNDO method. The HOMO and LUMO electronic density distributions of these molecules were plotted in Fig. 10. From this Figure it can be observed that the HOMO resides on the two oxygens of a

carboxylate ion group of the studied compounds, but the LUMO resides on the protonated amine group. The Mulliken charge densities of the amino acids have been calculated and presented in Figure 10. There is a general consensus by several authors that the more negatively charged heteroatom, the more it can be adsorbed on the metal surface through donor-acceptor type reaction [63, 64]. From the values of Mulliken charge we can observe the presence of excess of negative charge on nitrogen and oxygen atoms and hence the amino acids molecules can be adsorbed on Cu10Ni alloy surface using these active centers leading to the corrosion inhibition action.

Table 7 - The calculated quantum chemical parameters of the studied amino acids

Parameters	valine	alanine	glycine
E_{HOMO} (eV)	-10.79	-10.81	-10.98
E_{LUMO} (eV)	0.712	0.710	0.920
ΔE (eV)	11.5	11.52	11.90
Dipole moment (μ) (Debye)	1.12	1.13	2.16
Molecular weight	117.15	89.09	75.07

Table 7 shows the quantum chemical calculation parameters (E_{HOMO} , E_{LUMO} , ΔE ($E_{LUMO} - E_{HOMO}$), dipole moment (μ), heat of formation and ionization potential) which have been calculated and correlated with experimental results. From this Table it is evident that a correlation exists between E_{HOMO} and inhibition efficiency of the amino acids. The less negative E_{HOMO} and the smaller ΔE reflect a great inhibition efficiency of the studied inhibitors [65, 58]. From the energy of highest occupied molecular orbital (E_{HOMO}), the order of inhibition efficiency is as follow: valine > alanine > glycine

This is in a good agreement with the above mentioned experimental data obtained by potentiodynamic polarization, EIS and EFM techniques.

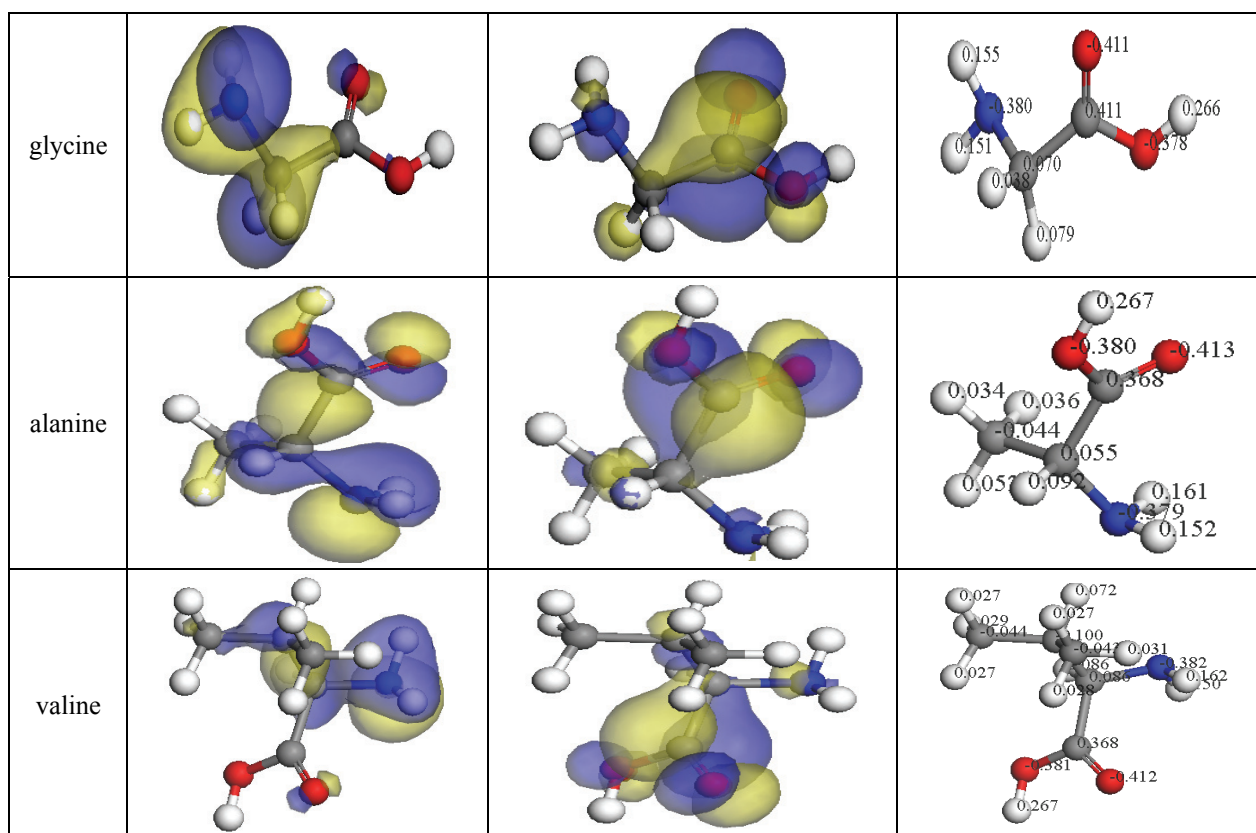


Figure 10 - Molecular orbital plots and Mulliken charges of valine, alanine and glycine using MNDO

4. CONCLUSIONS

The main conclusions drawn from this study are:

- valine, alanine and glycine inhibit the corrosion of Cu10Ni alloy in sulfide polluted salt water solutions.
- The Tafel plots of the inhibitors indicate that these compounds act as mixed-type inhibitors.
- The presence of KI improves the inhibition efficiency, indicating that there is a synergistic effect between these amino acids and the iodide anion.
- The inhibition is due to the physical adsorption of the inhibitor molecules on the Cu10Ni alloy surface.
- Adsorption of the inhibitors gives a good fit to Langmuir isotherm model.
- Results obtained from potentiodynamic polarization, ac impedance and EFM techniques are in good agreement and show increased inhibitor efficiency with increasing inhibitor concentration.
- From quantum chemical calculations, valine has the highest inhibition efficiency as compared to ala and glycine because it has the highest HOMO energy and lowest value of energy gap, ΔE ($E_{LUMO} - E_{HOMO}$).

REFERENCE

- [1] A.H.Tuthill, Mater. Perform., 26 (1987) 12.
- [2] R.F.North and M.I.Pryor, Corros. Sci., 10 (1970) 197.
- [3] C.W.Yeow, D.B.Hibbert, J. Electrochem. Soc., 130 (1983) 786.
- [4] G.Bianchi, P.longi, Corros. Sci., 13 (1973) 853.
- [5] J.P.Gudas, and H.P.Hack, Corros., 35(1979)167.
- [6] T.S. Lee, H.P. Hack and D.G. Tipton, Proceedings of the 5th International Congress on Marine Corrosion and Fouling, 1980.
- [7] D.D.Macdonald, B.C.Syrett, S.S.Wing, Corrosion 35 (1979) 367.
- [8] A. El. Domiaty and J.N. Alhajji, J. Mat. Eng. Perf., 6 (1997) 534.
- [9] S. M. Sayed, E.A. Ashour and G.I. Youssef, Mater. Chem. Phys., 78 (2003) 825.
- [10] S.M. Sayed, E.A. Ashour, G.I. Youssef, G.I. and S. M. El-Raghy, Egyptian J. Chem., 47(2) (2004) 157.
- [11] E.A. Ashour, J. Mater. Sci., 36 (2001) 201.
- [12] S. M. Sayed, E.A. Ashour, G.I. Youssef, S. M. El-Raghy, J. Mater. Sci., 37 (2002) 2267.
- [13] J. Wang, X. Jiang, X. and S. Li, J. Chinese Soc. Corros. Prot., 17(2) (1997) 85.

- [14] E. M.Sherif, S. M. Park, *Electrochim. Acta*, 51 (2006) 4665.
- [15] N.K. Allam and E.A. Ashour, *Mat. Sci. Eng. B*, 156 (2009) 84.
- [16] N. K. Allam, A. Abdel-Nazeer, and E. A. Ashour, *J. Appl. Electrochem.*, 39 (2009) 961.
- [17] N. K. Allam, E. A. Ashour, H. S. Hegazy, B. E. El-Anadolli, and B. G. Ateya, *Corros. Sci.*, 47 (2005) 2280.
- [18] S.M.Sayed, E.A.Ashour and B.G.Ateya, *Corros. Sci.*, 36 (1994) 221.
- [19] N. K. Allam and E. A. Ashour, *Appl. Surf. Sci.*, 254 (2008) 5007.
- [20] M.Ehteshamzadeh, T.Shahrabi, M.G.Hosseini, *J. Appl. Surf. Sci.*, 252 (2006) 2949.
- [21] N. K. Allam H. S. Hegazy and E. A. Ashour, *J. Electrochem. Soc.*, 157 (2010) 174.
- [22] G.Moretti, F.Guidi, *Corros. Sci.* 44 (2002) 1995.
- [23] E.Stupnisek-Lisac, N.Galic, R. Gasparac, *Corrosion* 56(2000)1105.
- [24] E.Stupnisek-Lisac, A.Gazivoda, M.Modzarac, *Electrochim. Acta* 47 (2002) 4189.
- [25] H.Ashassi-Sorkhabi, Z.Ghasemi, D.Seifzadeh, *Appl. Surf. Sci.* 249 (2005) 408.
- [26] W.A.Badawy, K.M.Ismail, A.M.Fathi, *Electrochim. Acta* 51 (2006) 4182.
- [27] K.F.Khaled, *Mat. Chem. Phys.* 112 (2008) 104.
- [28] K.M.Ismail, *Electrochim. Acta* 52 (2007) 7811.
- [29] E.Rocca, G.Bertrand, C.Rapon, J.C.Labrunie, *J. Electroanal.* 503 (2001) 133.
- [30] S.A.Abd El-Maksoud, *Electrochim. Acta* 49 (2004) 4205.
- [31] S.Varvara, L.M.Muresan, K.Rahmouni, H. Take-nouti, *Corros. Sci.*, 50 (2008) 2596.
- [32] E.E.Oguzie, Y.Li, F.H.Wang, *J. Colloid Interface Sci.* 310(2007) 90.
- [33] M.M. El-Rabiee, N.H. Helal, Gh.M. Abd El-Hafez, W. A. Badawy, *J. Alloys. Compounds.* 459 (2008) 466.
- [34] Da-Quan Zhang, Qi-Rui Cai, Li-Xin Gao, Kang Yong Lee, *Corros. Sci.* 50 (2008) 3615.
- [35] A. Aksut, S. Bilgic, *Corros. Sci.* 33 (1992) 379.
- [36] Da-Quan Zhang, Qi-Rui Cai, Xian-Ming He, Li-Xin Gao, Gui Soon Kim, *Mater. Chem. Phys.* 114 (2009) 612.
- [37] G. Gomma, H. Wahdan, *Mater. Chem. Phys.* 39 (1994) 142.
- [38] M. Rylkina, A. Chikanova, L. Trubacheva, S. Reshetnikov, *Protection of Metals* 35 (1999) 23.
- [39] H. Baba, T. Kodama, *Corros. Sci.* 41 (1999) 1987.
- [40] Da-Quan Zhang, Qi-Rui Cai, Xian-Ming He, Li-Xin Gao, Guo-Ding Zhou, *Mater. Chem. Phys.* 112 (2008) 353.
- [41] W. A. Badawy, K.M.Ismail, A. M. Fathi, *J. Appl. Electrochem.* 35 (2005) 879.
- [42] E.E.Oguzie, Y.Li, F.H.Wang, *Electrochim. Acta* 53 (2007) 909.
- [43] D. Kalota, D. Silverman, *Corros. Sci.* 50 (1994) 138.
- [44] G.Gomma, *Bull. Electrochem.* 12 (1998) 456.
- [45] L.Madkour, M.Ghoneim, *Bull. Electrochem.* 13 (1997) 1.
- [46] R.G. Lakshmi, *Electrochemical and wear behavior of surface modified orthopaedic titanium alloys*, Ph.D. Thesis, Anna University, India, 2003.
- [47] B. Ramesh Babu, R. Holze, *Br. Corros. J.* 35 (2000) 204.
- [48] G. Bereket, A. Yurt, *Corros. Sci.* 43 (2001) 1179.
- [49] G.P. Cicileo, B.M. Rosales, F.E. Varela and J.R. Vilche, *Corros. Sci.* 40 (1998) 1915.
- [50] A. Popova, M. Christov, *Corros. Sci.* 48 (2006) 3208.
- [51] C.H. Hsu, F. Mansfeld, *Corrosion* 57 (2001) 747.
- [52] W.A. Badawy, K.M. Ismail, and A.M. Fathi, *J. Appl. Electrochem.* 35 (2005) 879.
- [53] M. Bethencourt, F.J. Botana, J.J. Calvino, M. Marcos, *Corros. Sci.* 40 (1998) 1803.
- [54] Gamry Echem Analyst Manual, 2003.
- [55] E. Khamis, *Corros.* 46 (1990) 476.
- [56] M. Hosseini, S.F.L. Mertens, M.R. Arshadi, *Corros. Sci.* 45 (2003) 1473.
- [57] E.E. Oguzie, *Corros. Sci.* 49 (2007) 1527.
- [58] G. Gece, *Corros. Sci.* 50 (2008) 2981.
- [59] K. Fukui, *Theory of Orientation and Stereoselection*, Springer-Verlag, New York, 1975.
- [60] H. Ashassi-Sorkhabi, B. Shaabani and D. Seifzadeh, *Electrochim. Acta* 50 (2005) 3446.
- [61] M. Ozcan, I. Dehri and M. Erbil, *Appl. Surf. Sci.* 236 (2004) 155.
- [62] N. Khalil, *Electrochim. Acta* 48 (2003) 2635.
- [63] W. Li, Q. He, C. Pei, B. Hou, *Electrochim. Acta* 52 (2007) 6386.
- [64] I.B. Obot, N.O. Obi-Egbedi, S.A. Umoren, *Corros. Sci.* 51 (2009) 276.
- [65] G. Gece, S.Bilgic, O.Turksen, *Mat. and Corros.* 60 (2009) 9999.